THE ASTROPHYSICAL JOURNAL, 520:L115–L118, 1999 August 1

DUST EMISSION FROM HERBIG Ae/Be STARS: EVIDENCE FOR DISKS AND ENVELOPES

ANATOLY MIROSHNICHENKO,[1] ŽELJKO IVEZIĆ,[2] DEJAN VINKOVIĆ,[3] AND MOSHE ELITZUR[3,4]

Received 1999 April 13; accepted 1999 May 26; published 1999 June 23

ABSTRACT

Infrared and millimeter-wave emission from Herbig Ae/Be stars has produced conflicting conclusions regarding the dust geometry in these objects. We show that the compact dimensions of the millimeter-wave–emitting regions are a decisive indication for disks. But a disk cannot explain the spectral energy distribution unless it is embedded in an extended envelope that (1) dominates the IR emission and (2) provides additional disk heating on top of the direct stellar radiation. Detailed radiative transfer calculations based on the simplest model for envelope-embedded disks successfully fit the data from UV to millimeter wavelengths and show that the disks have central holes. This model also resolves naturally some puzzling results of IR imaging.

Subject headings: accretion, accretion disks — circumstellar matter — dust, extinction — stars: pre–main-sequence

1. INTRODUCTION

Attempts at determining the dust geometry around Herbig Ae/Be (HAEBE) stars from IR and millimeter-wave data have yielded conflicting conclusions. From the shape of the spectral energy distribution (SED), Hillenbrand et al. (1992) suggested that the IR emission from 30 HAEBE stars is dominated by optically thick accretion disks. However, Miroshnichenko, Ivezić, & Elitzur (1997, hereafter MIE) successfully modeled the detailed data of eight of these objects with optically thin spherical envelopes in free fall. Worse yet, occasionally the data at different wavelengths from the same source seem in conflict. Mannings & Sargent (1997, hereafter MS) measured the millimeter-wave emission from seven HAEBE stars, including two of the MIE sources. They find that the visual optical depths (τ_V) required to explain the millimeter emission with the MIE models are at least 220, at considerable odds with the small *V*-band extinction of each source. In particular, MIE successfully fitted all $\lambda \leq 100$ μm data with $\tau_V = 0.4$ for MWC 480 and $\tau_V = 0.3$ for MWC 863, yet MS find that within the context of the MIE model, the millimeter emission from these sources requires $\tau_V > 10^3$ and $\tau_V = 601$, respectively. Based on imaging and CO line observations, MS infer substantial disk components for their entire sample. However, emission from optically thick accretion disks yields similar inconsistencies. In this case, $F_\nu \propto \nu^{1/3}$, and extrapolating the flux from the MS millimeter measurements produces IR emission that is more than an order of magnitude too weak. For example, for MWC 863 the measured 2.6 mm flux of 13.7 mJy extrapolates to only 0.1 Jy at 2.2 μm, where the observed flux is 4.6 Jy. Also, the proposed accretion disks would be optically thick at 10 μm, where the silicate feature indicates prominent optically thin emission in most of the MS sources.

Similar inconsistencies arise from the HAEBE star imaging by Di Francesco et al. (1994, hereafter DF). Irrespective of geometry, the longer the radiation wavelength, the cooler the emitting region is, and since temperature drops with distance from the center, the image size should increase with wavelength. While this was the case for most sources, the image size of MWC 137 was $66'' \pm 2''$ at 50 μm and only $58'' \pm 2''$ at 100 μm. No single dust configuration can produce a decrease of observed size with wavelength.

We propose a simple solution to the internal inconsistencies that seem to afflict the observations at different wavelengths of some HAEBE stars: the dust distribution in these sources has both an extended spherical component, dominating the IR emission, and an embedded compact disk which dominates the millimeter and submillimeter emission. Here we show that this simple model resolves all the conflicts quite naturally.

2. MODELING AND RESULTS

The system consists of a star of radius R_* and effective temperature T_*, surrounded by a geometrically thin and optically thick passive disk extending from R_* to some outer radius $R_{\rm disk}$. In addition, a spherical dusty envelope starts at the radius $R_{\rm sub}$, which corresponds to dust sublimation. We have analyzed this system with the aid of the scaling theory of Ivezić & Elitzur (1997) and the classical accretion disk theory as adapted to T Tauri stars by Bertout, Basri, & Bouvier (1988). Details of our analysis will be reported elsewhere. Here we present detailed model calculations, performed with the code DUSTY[5] (Ivezić, Nenkova, & Elitzur 1997), that successfully fit the SEDs of all the stars in the MS sample.

Our modeling procedure is similar to MIE except that each model flux is the sum of disk and envelope contributions, where the latter includes also the attenuated stellar emission. For any flux distribution F_λ, we introduce the dimensionless, normalized SED $f_\lambda = \lambda F_\lambda / \int F_\lambda d\lambda$, which depends only on dimensionless quantities—luminosities, densities, and linear dimensions are irrelevant (Ivezić & Elitzur 1997). The only relevant property of the stellar radiation is its spectral shape, taken from the appropriate Kurucz (1994) model atmosphere. For the dust, the only relevant properties are the spectral shapes of the absorption and scattering coefficients, which we take from standard interstellar mix, and the sublimation temperature, which we take as $T_{\rm sub} = 1500$ K. DUSTY performs a self-consistent calcu-

[1] Pulkovo Observatory, St. Petersburg 196140, Russia; anat@pulkovo.spb.su.

[2] Princeton University, Department of Astrophysical Sciences, Princeton, NJ 08544; ivezic@astro.Princeton.edu.

[3] Department of Physics and Astronomy, University of Kentucky, Lexington, KY 40506; dejan@pa.uky.edu, moshe@pa.uky.edu.

[4] Service d'Astrophysique, Centre d'Études de Saclay, 91190 Gif-sur-Yvette, France.

[5] Accessible at http://www.pa.uky.edu/~moshe/dusty.

TABLE 1
PROPERTIES OF MODELED SYSTEMS

Name (1)	Spectral Type (2)	A_V (3)	ρ (4)	τ_V (5)	p (6)	$T_{\rm disk}^{\rm out}$ (7)	$\tau_{\rm disk}^{350}$ (8)	$\theta_{\rm disk}$ (9)	$R_{\rm sub}/R_*$ (10)
AB Aur	A0	0.2	0.21	0.5	2*	25	0.9	2.5	98
MWC 480	A3	0.4	0.14	0.25	2	20	18	2.0	88
HD 245185	A0	0	0.14	0.6	1	25	2	1.8	91
CQ Tau	A8	0.1	0.17	2.7	1	30	5	2.6	79
MWC 863	A3	1.2	0.05	0.45	2	40	>50	1.0	90
HD 163296	A3	0.3	0.17	0.3	2	20	20–30	3.1	94
MWC 758(A)	A8	0.2	0.49	0.25	0.5	45	1.4	0.5	78
MWC 758(B)	A8	0	0.67	0.2	1.5	45	2	0.3	79

NOTE.—Col. (2) lists the spectral type used in the modeling; for all other properties of the stars, see Mannings & Sargent 1997. Cols. (3)–(8) list the parameters determined from modeling. Overall parameters are the interstellar extinction to the system (col. [3]) and the fractional contribution of the disk to the bolometric flux (col. [4]). The envelope parameters are its overall optical depth at visual (col. [5]) and the power of its density profile y^{-p} ($y = r/R_{\rm sub}$) (col. [6]), which is terminated at $y = 1000$. The only exception is AB Aur (*asterisk*), whose envelope is modeled with a broken power law: $p = 2$ for $1 \leq y \leq 100$ and $p = 0$ for $100 < y \leq 5000$. The disk parameters are its temperature (in K) (col. [7]) and 350 μm optical depth at the outer edge (col. [8]). Derived properties are the disk observed diameter (in arcseconds) (col. [9]) and the envelope inner radius (col. [10]).

lation of the temperature profiles[6] of the disk and the envelope, taking into account both the scattered and attenuated stellar radiation and diffuse envelope emission; the effect of disk emission on the envelope temperature is negligible for the parameters considered here. The envelope SED $f_{{\rm env},\lambda}$ is determined by the envelope optical depth τ_V and the dimensionless profile of its density distribution in terms of $y = r/R_{\rm sub}$, where r is distance from the star. Here we employ the simple profile y^{-p}, with p as a free parameter, extending from $y = 1$ to some $y = Y$. If shadowing by the star is neglected, then $F_{{\rm disk},\lambda} \propto \cos i$, where i is the disk inclination angle, and the disk SED $f_{{\rm disk},\lambda}$ is independent of i. The disk is assumed to be optically thick everywhere at the peak of the Planckian with the local temperature. Then $f_{{\rm disk},\lambda}$ has only two free parameters—the temperature and normal optical depth of the disk outer edge, which we denote $T_{\rm disk}^{\rm out}$ and $\tau_{\rm disk}^{350}$, respectively, the latter specified at 350 μm. Once $f_{{\rm disk},\lambda}$ and $f_{{\rm env},\lambda}$ are computed, the observed SED is fitted through $f_\lambda = \rho f_{{\rm disk},\lambda} + (1 - \rho) f_{{\rm env},\lambda}$, where $\rho = F_{\rm disk}/(F_{\rm disk} + F_{\rm env})$ is a free parameter. The final free parameter is A_V, the interstellar extinction to the system.

Figure 1 shows our modeling results, including all available data from 1400 Å to 2.7 mm. In addition to the *IRAS* Low-Resolution Spectrometer (LRS) data when available, the plot for each object contains 20–30 data points from various sources. The model parameters obtained for each star are listed in Table 1. It is worth noting that the A_V's we find are similar to those derived by MS. As is evident from the figure, envelopes with a simple power-law density distribution adequately fit almost all sources. In all those cases, the figure displays the model with $Y = 1000$, but there is considerable freedom in this parameter and successful models can be constructed with Y as small as ~150. In addition, acceptable fits can be obtained when the power p is reduced by as much as 0.5 in most cases. The largest freedom exists for MWC 758, which lacks LRS data, and we present the two models that bracket the range of p; any value in between is possible. The one exception is AB Aur, this sample's most luminous object, which requires an extended envelope ($Y = 5000$) with a broken power-law density profile. Indeed, it is the only source in this sample surrounded by a visible nebulosity (Herbig 1960); the nebulosity size (~1.′5) agrees with our model requirements. A flattening of the density distribution away from the center can be expected at the late evolutionary stages of collapsing clouds (e.g., Shematovich, Shustov, & Wiebe 1997).

The key to the resolution of the conflicts outlined above is the great disparity between the disk and envelope temperature profiles. While heating by stellar radiation produces disk temperature that varies as $r^{-3/4}$, the envelope temperature decreases only as $r^{-0.36}$ for dust opacity $\propto\lambda^{-1.5}$. As a result, the disk is much cooler than the envelope at all radii at which both exist and can also contain cooler material in spite of being much smaller. Both properties are evident from the top panel of Figure 2, which shows the temperature profiles of the two components in AB Aur. Natta (1993) pointed out that heating by the spherical dusty envelope significantly affects the disk temperature, and our calculations confirm this important point. In Figure 1, the first bump (around 1 μm) in each disk emission reflects the stellar heating; the second is produced by the envelope heating. But this does not alter the fundamental difference between the temperature profiles of the two components, as the AB Aur case shows. Although it is more compact, the disk can be the stronger emitter at long wavelengths so that the SED is dominated by the envelope at IR wavelengths and by the disk at millimeter wavelengths. This is the case for all sources in Figure 1.

This role reversal affects also the wavelength behavior of images. At shorter wavelengths the image is dominated by the envelope, and the observed size increases with wavelength. When the SED switches to disk domination, the observed size can decrease because a given temperature occurs on the disk at a much smaller radius than in the envelope. This effect is evident in Figure 2, which shows the surface brightness profiles of the AB Aur model at various wavelengths. These profiles agree well with imaging observations (DF; Marsh et al. 1995; MS). The finite beam size and dynamic range of any given telescope could result in an apparent size decrease between 10 and 100 μm in this case. A switch from envelope to disk domination provides a simple explanation for the otherwise puzzling decrease in the observed size of MWC 137 between 50 and 100 μm. A similar effect was recently detected also in the dust-shrouded main-sequence star Vega. Van der Bliek, Prusti, & Waters (1994) find that its 60 μm size is $35'' \pm 5''$, yet 850 μm imaging by Holland et al. (1998) produced a size

[6] There is no need to consider stochastic heating of very small grains. The stellar radiation field is sufficiently intense that all grains are in thermal equilibrium with it (A. Jones 1999, private communication).

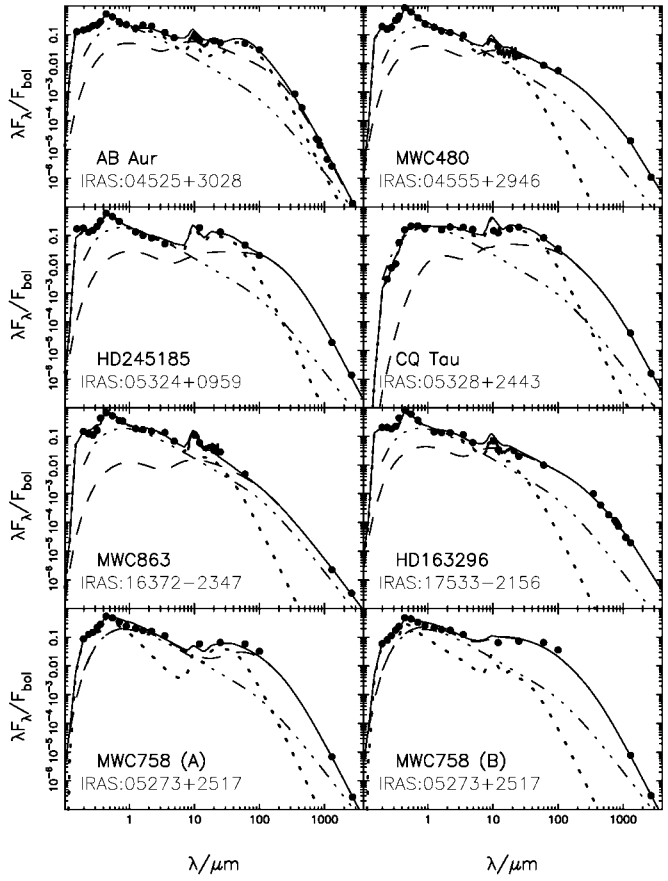

FIG. 1.—Fits to the SEDs of the MS sources with models comprised of geometrically thin, optically thick disks embedded in spherical dusty envelopes. The data (dereddened with the A_V listed in Table 1) are marked with points, and LRS data (when available) are marked with thick lines in the 8–24 μm range. Each model SED (*full line*) is the sum of the contributions of the envelope (*dotted line*) and disk (*dashed line*) whose parameters are listed in Table 1. The dash-dotted line in each panel is the SED that a face-on disk would produce if the envelope did not exist.

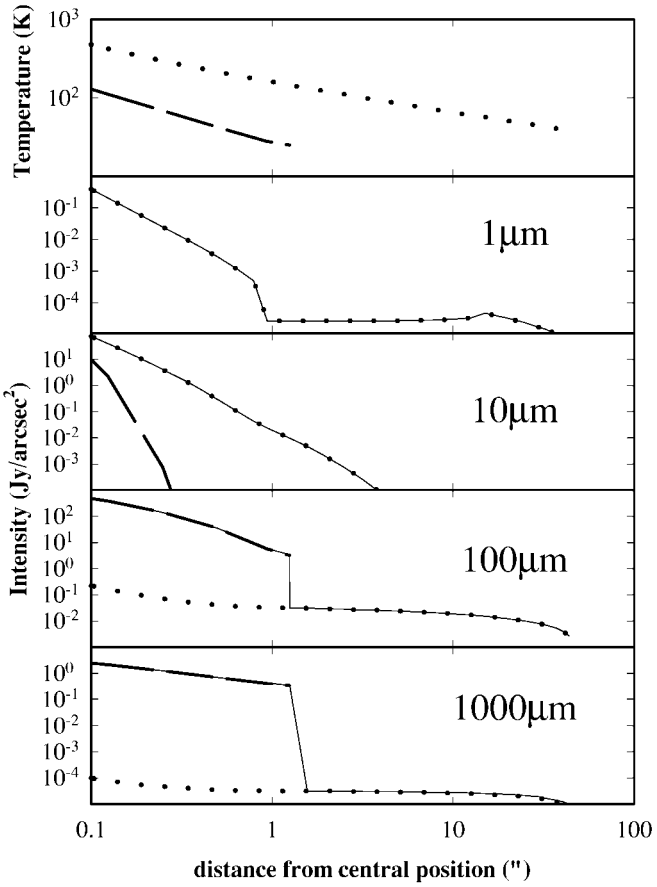

FIG. 2.—Variation of temperature (*top panel*) and intensity at various wavelengths with distance from the center along the apparent major axis of the tilted disk for the AB Aur model (see Table 1; at the nominal distance to this source, 0″.1 ≃ 15 AU). In each panel, the dotted line corresponds to the envelope, and the dashed line corresponds to the disk. In the lower four panels, the overall intensity (*full line*) is the sum of the contributions of the two components. Note the role reversal of the two intensity components between 10 and 100 μm.

of only 24 × 21″ ± 3″. So the dust distribution around Vega, too, could have both spherical and disk components.

3. DISCUSSION

Our models successfully fit the entire MS sample, resolving all the earlier discrepancies. Both disk and envelope are crucial components. A purely spherical distribution could successfully fit each SED, but the cool millimeter-wave–emitting material would have to be placed about 100 times farther from the star than the MS observations indicate (an example is the recent spherical fit for AB Aur by Henning et al. 1998). The compact millimeter-wave emission observed from these sources can be produced only by the "classic" geometrically thin, optically thick disks, as correctly recognized by MS. But such disks alone are incapable of explaining the observations. This is evident from Figure 1, which shows the maximum possible emission from this configuration, obtained when a "bare" disk is observed face-on. In all sources this emission falls short of observations at $\lambda \gtrsim 5$ μm, mostly by substantial amounts. The envelope is essential not only for its direct IR flux which dominates the observations at these wavelengths, but also for its indirect effect on the submillimeter and millimeter-wave emission, which is disk dominated; the observations at these wavelengths cannot be explained without the additional disk heating by the envelope.

Our detailed model results depend on the simplifying assumptions, but the main conclusions seem robust: the density distribution contains two distinct components, one optically thick, cool, and compact, the other optically thin, warmer, and more extended. The spherical idealization is not essential for the latter, since the envelopes can be flattened and even distorted into irregular shapes before severely affecting the results. Recently Chiang & Goldreich (1997, hereafter CG) pointed out that the optically thin emission from the surface layer of an optically thick disk can significantly affect the SED, and in principle this layer could fulfil the role of the envelope advocated here. However, the emission from the CG layer can be shown equivalent to that from a spherical envelope with optical depth $\tau_V = 0.8R_*/R_{\rm sub}$ and density profile $p = 2$ for $y < 6$ and $p = 5/7$ thereafter. Detailed model calculations with these equivalent envelopes show that they cannot fit the MS sources. In particular, all the MS sources require $\tau_V > 0.1$ for their observed fluxes, but only have $R_*/R_{\rm sub} \sim 0.01$ (Table 1); i.e., the column of optically thin dust contained in the disk surface layer is only ~10% of what the observations require, and we are justified in neglecting this layer in our model calculations of HAEBE stars. On the other hand, in T Tau stars,

the subject of the CG study, R_*/R_{sub} is an order of magnitude larger than for HAEBE stars (because T_* is lower) and the surface layer becomes a significant component. The MS sources HD 245185 and MWC 758 are potential exceptions because good fits to their SEDs are possible with rather flat density profiles and modest optical depths. Such envelopes could be made equivalent to CG layers if the parameters of the CG model are scaled to the HAEBE star environment keeping the basic assumptions intact. Settling the issue with certainty for these two cases requires a two-dimensional radiative transfer code, which we are currently developing. In all other sources, our conclusion about the negligible role of the disk surface layer seems secure.

Almost all the envelopes have $\tau_V < 1$; therefore, their material is largely atomic. With standard dust abundance, the envelope column densities are $\sim 10^{20}$ cm^{-2}. All stars in this sample have $R_* \sim 2\ R_\odot$; therefore, $R_{sub} \sim 10^{13}$ cm and the densities at the envelope inner regions are $\sim 10^7$ cm^{-3}. In contrast with MS, the DF selection criterion was high luminosities. Since R_{sub} scales with $L^{1/2}$, the DF sources should have more extended envelopes, as observed. The envelope mass strongly depends on its outer radius, and this parameter is rather poorly constrained. With $Y = 1000$, which was employed in the displayed fits, envelope masses range from $\sim 10^{-4}\ M_\odot$ for the sources with $p < 2$ to $\sim 10^{-6}\ M_\odot$ for the sources with $p = 2$. However, these mass estimates decrease sharply for smaller values of Y, which are possible in all cases. The one exception is AB Aur, where there is little freedom in the outer radius, and the model parameters give an envelope mass of $0.03\ M_\odot$, the same as a recent estimate by Henning et al. (1998). The power $p = 2$ could indicate outflow with constant velocity; indeed, N v emission from AB Aur was recently modeled with a wind (Bouret, Catala, & Simon 1997). However, acceptable fits can be produced also with $p = 3/2$. If this index is interpreted as steady state accretion to a central mass, the envelope optical depths translate to accretion rates of $\sim 10^{-8}\ M_\odot$ yr^{-1}, similar to those deduced from UV spectra of HAEBE stars (Grady et al. 1996) and T Tau stars (Valenti, Basri, & Johns 1993; Gullbring et al. 1998). These low rates cannot correspond to the main accretion buildup of the star but rather a much later phase, involving small, residual accretion from the environment. The corresponding accretion luminosities are only $\sim 0.1\ L_\odot$, justifying their neglect in our calculations.

Since the disk is optically thick in our model, its density distribution remains undetermined and we cannot improve on the MS estimates of disk masses ($\sim 10^{-2}\ M_\odot$). Useful information can be deduced from the parameter ρ because it is easy to show that $\rho = 2x \cos i/(1 - x + 2x \cos i)$, where x is the disk fractional contribution to the overall luminosity. Our calculations automatically determine x in each case, allowing us to deduce i from the model fit for ρ. If the disk extends all the way to the stellar surface, then $x = 0.4$ for the AB Aur model[7] which translates to $i = 80°$ for this source, similar to the 76° that MS deduced from the disk elliptical appearance. However, following the same procedure for all other stars produces $i > 80°$ in each case. Since an edge-on orientation for every single disk in this sample is highly unlikely, we conclude that x cannot be as large as this procedure implies for all the systems. Indeed, central holes would drastically reduce x because of the steep dependence of disk luminosity on the radius of the disk inner edge. Moving this edge from R_* to only $2R_*$ removes 56% of the stellar luminosity intercepted by the disk; $3R_*$ results in a 72% removal. Central holes of virtually any size would sharply decrease x, resulting in a more plausible distribution of inclination angles. Such holes would not impact any other model result because they remove only the hottest disk material whose contribution to the observed flux is negligible in all cases. The sizes of these holes cannot be determined from the modeling, but their existence seems an unavoidable conclusion.

The discrepancies among previous studies of HAEBE stars underscore the importance of combining multiwavelength data in an integrative approach. Single-wavelength observations, however detailed, never fully reconstruct the geometry of dust distribution. At $\lambda \lesssim 3\ \mu$m, the observed radiation is scattering dominated because dust emission would require temperatures higher than sublimation. Scattered photons trace the density distribution, so images at these wavelengths reveal the actual geometry—but only close to the center, to scattering optical depth ~1. In contrast, radiation at longer wavelengths can map much farther regions because it is dominated by dust emission. However, the emission is predominantly governed by the dust temperature distribution, which primarily reflects distance from the central star and thus tends to be spherically symmetric even when the density distribution is not. By example, images of the nebulosity around the late-type star IRC +10216 are elongated at $\lambda \lesssim 3$–$4\ \mu$m yet spherically symmetric at longer wavelengths (Ivezić & Elitzur 1996). Recent NICMOS images of young stellar objects show complex morphologies (Padgett et al. 1999), and there is no reason to believe they should be simpler for HAEBE stars. Nevertheless, resolving such details does not alter the measured SED. The model parameters deduced here can be expected to provide a reasonable description of the envelope properties when small-scale structure is averaged out.

We would like to thank A. Jones for useful discussions of small-grain heating. Support by NASA, NSF, CEA, and CNRS is gratefully acknowledged.

[7] A "bare" disk that extends to the stellar surface has $x = 0.25$.

REFERENCES

Bertout, C., Basri, G., & Bouvier, J. 1988, ApJ, 330, 350
Bouret, J.-C., Catala, C., & Simon, T. 1997, A&A, 328, 606
Chiang, E. I., & Goldreich, P. 1997, ApJ, 490, 368 (CG)
Di Francesco, J., Evans, N. J., II, Harvey, P. M., Mundy, L. G., & Butner, H. M. 1994, ApJ, 432, 710 (DF)
Grady, C. A., et al. 1996, A&AS, 120, 157
Gullbring, E., Hartmann, L., Briceño, C., & Calvet, N. 1998, ApJ, 492, 323
Henning, Th., Burkert, A., Launhardt, R., Leinert, Ch., & Stecklum, B. 1998, A&A, 336, 565
Herbig, G. H. 1960, ApJS, 4, 337
Hillenbrand, L. A., Strom, S. E., Vrba, F. J., & Keene, J. 1992, ApJ, 397, 613
Holland, W. S., et al. 1998, Nature, 392, 788
Ivezić, Ž., & Elitzur, M. 1996, MNRAS, 279, 1019
———. 1997, MNRAS, 287, 799
Ivezić, Ž., Nenkova, M., & Elitzur, M. 1997, User Manual for DUSTY, Univ. Kentucky Internal Rep.
Kurucz, R. L. 1994, CD-ROM 19, Solar Abundance Model Atomospheres for 0, 1, 2, 4, 8 km/s (Cambridge: SAO)
Mannings, V., & Sargent, A. I. 1997, ApJ, 490, 792 (MS)
Marsh, K. A., Van Cleve, J. E., Mahoney, M. J., Hayward, T. L., & Houck, J. R. 1995, ApJ, 451, 777
Miroshnichenko, A., Ivezić, Ž., & Elitzur, M. 1997, ApJ, 475, L41 (MIE)
Natta, A. 1993, ApJ, 412, 761
Padgett, D. L., Brandner, W., Stapelfeldt, K. R., Strom, S. E., Terebey, S., & Koerner, D. 1999, AJ, 117, 1490
Shematovich, V. I., Shustov, B. M., & Wiebe, D. S. 1997, MNRAS, 292, 601
Valenti, J. A., Basri, G., & Johns, C. M. 1993, AJ, 106, 2024
van der Bliek, N. S., Prusti, T., & Waters, L. B. F. M. 1994, A&A, 285, 229